J. Phys. D: Appl. Phys. **41** (2008) 215405 (11pp) doi:10.1088/0022-3727/41/21/215405

The static actuation of dielectric elastomer actuators: how does pre-stretch improve actuation?

Guggi Kofod

University of Potsdam, Institute of Physics, Advanced Condensed-Matter Physics, 14476 Potsdam, Germany

E-mail: guggi.kofod@uni-potsdam.de

Received 23 July 2008, in final form 10 September 2008
Published 13 October 2008
Online at stacks.iop.org/JPhysD/41/215405

Abstract

It has previously been shown that providing dielectric elastomer actuators with a level of pre-stretch can improve properties such as breakdown strength, actuation strain and efficiency. The actuation in such actuators depends on an interplay between the highly nonlinear hyperelastic stress–strain behaviour with the electrostatic Maxwell's stress; however, the direct effects of pre-stretch on the electromechanical coupling have still not been investigated in detail. We compare several experimental results found in the literature on the hyperelastic parameters of the Ogden model for the commonly used material VHB 4910, and introduce a more detailed and thus more accurate fit to a previous uniaxial stress–strain experiment. Electrostatic actuation models for a pure shear cuboid dielectric elastomer actuator with pre-stretch are introduced, for both intensive and extensive variables. For both intensive and extensive variables the constant strain (blocked stress or force) as well as the actuation strain is presented. It is shown how in the particular case of isotropic amorphous elastomers the pre-stretch does not affect the electromechanical coupling directly, and that the enhancement in actuation strain due to pre-stretch occurs through the alteration of the geometrical dimensions of the actuator. Also, the presence of the optimum load is explained as being due to the plateau region in the force–stretch curve, and it is shown that pre-stretch is not able to affect its position. Finally, it is shown how the simplified Ogden fit leads to entirely different conclusions for actuation strain in terms of extensive variables as does the detailed fit, emphasizing the importance of employing accurate hyperelastic models for the stress–stretch behaviour of the elastomer.

1. Introduction

Linear actuators with output properties similar to that of biological muscle could have an immense impact on areas such as industrial and personal robotics, orthopaedic assists and medical devices in general. A promising class of linear actuators, known as electroactive polymer actuators [1], are based on large deformations in polymer materials that can arise due to electrically induced changes in electrochemical, thermal or electrostatic energy. One of these actuator technologies, the dielectric elastomer actuators, are known to possess useful output properties, with obvious advantages in ease of use, scope of applicability, cost and reliability [2].

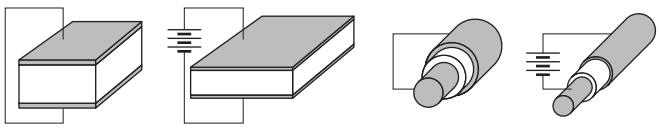

Figure 1. Actuation in dielectric elastomer actuators, planar (left) and co-axial (right).

Dielectric elastomer actuators can be thought of as rubber capacitors [3] (planar or co-axial, see figure 1) which can convert electrical into mechanical energy and vice versa. This electromechanical coupling may result in actuation strains on the order of several hundred per cent, with actuation pressures similar to that of biological muscle; however, usually several

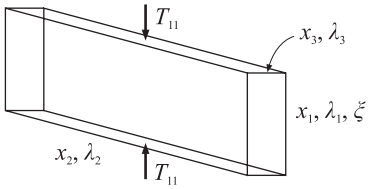

Figure 2. Cuboid geometry, with indication of naming convention. The actuation strain ξ is defined in (3) and (4).

kilovolts are required to reach such levels [4, 5]. For a prediction of the properties of a dielectric elastomer actuator undergoing very large stretches, it is necessary to depart from models based on linear stress–stretch. Indeed, the stress–stretch behaviour should be modelled with hyperelastic models in order to capture the full functionality.

It has been shown that the output properties of an actuator structure based on dielectric elastomers can be improved by incorporating *pre-stretch*, which corresponds to stretching the elastomer during manufacture of the actuating structure, and ensuring that some level of pre-stretch remains during actuation [5–9]. Only the parts of the elastomer film which remain freestanding will provide actuation forces, which can then be used to deform the entire structure of elastomer and frame. Examples of this approach are provided by the spring-roll actuator [10] which was used in an arm wrestling application [9], the bi-stable diamond actuator loaded with a spring frame [11] or with a rubber band [12], the minimum energy structure actuator [13] and the actuating shell actuator used for a swimming blimp application [14].

The structure and results of the analysis will depend upon the choice of geometry and the applicable boundary conditions. Many actuator geometries have been analysed already; however, it is typically the case that the complications of the geometry obscure the effects that a good choice of material would have on the overall actuator performance. Here, the simple cuboid geometry is chosen (figure 2). For this geometry the stress and strain fields are constant and the analysis can be completed analytically, without the use of finite element modelling.

It has been shown that pre-stretch has the effect of improving actuator performance tremendously [5, 6], which can be partially explained by the observed increase in breakdown strength [7, 12]. The increase in breakdown strength was attempted explained by a thermodynamic stability criterion [15]. The effects of pre-stretch on the actuation properties of dielectric elastomer actuators have been investigated [4–8, 10, 12–14, 16–22]; however, a detailed analysis of the impact of pre-stretch on electromechanical coupling in a cuboid dielectric elastomer actuator has not been presented.

This study aims to show the effects of pre-stretch on the actuation behaviour of a simple cuboid dielectric elastomer actuator (figure 2). A proper analysis of these highly nonlinear effects is possible only through the use of graphical representation. For this geometry, all mechanical and electrical fields can be assumed constant throughout the dielectric elastomer, which helps to emphasize material property aspects of the actuation. The parameters involved in the model can be determined via independent measurements, as can the dimensions of the actuator. The choice of variables is, however, not obvious, and it is shown below how a given choice of variables may affect the conclusions which can be drawn from the analysis. Also, it is shown how the level of accuracy in the choice of hyperelastic modelling has a profound effect upon the predicted actuation properties.

2. Geometry and material parameters

Uniform actuation occurs when the stress and strain fields are constant throughout the elastomer, a condition which is provided by the cuboid actuator, as well as the diamond actuator [12]. Since the local actuation stress is proportional to the square of the electrical field, any irregularities in the uniform thickness will cause severe irregularities in local actuation and lead to reduced device actuation [23]. It is therefore to be expected that an analysis of actuator geometries that provide uniform electrical and mechanical fields will also allow for more accurate model predictions. The actuator geometry determines the elastic deformations of the actuator, which can be uniaxial, equi-biaxial, pure shear or other. The symmetry properties of these deformations lead to simplifications in the analytical expressions describing the deformation under actuation, which also applies to the cuboid actuator.

2.1. Geometry and boundary conditions

The coordinate axes for the description of the cuboid actuator are chosen with the 1-axis along the length of the actuator, the 2-axis along its width and the 3-axis along the thickness of the actuator (see figure 2). Initial dimensions of the actuator are designated x_i' and instantaneous dimensions by x_i, while the principal deformation ratios are defined as $\lambda_i = x_i/x_i'$. In the following, the principal deformation ratios λ_i are referred to as stretches.

It is assumed that (1) the deformation is isochoric and (2) the width of the actuator is always constant (corresponding to pure shear)

$$\lambda_1\lambda_2\lambda_3 = 1, \qquad \lambda_2 = \lambda_Q. \tag{1}$$

The isochoric constraint is a common choice in hyperelasticity which holds to a high degree for most elastomer materials. The fixed width assumption can be approximately realized by choosing a high aspect ratio between width and length, and between width and thickness ($x_2' \gg x_1'$ and $x_2' \gg x_3'$). The fixed stretch λ_Q in the width direction corresponds to the above mentioned *pre-stretch*. 'Pre-stretch' and 'width pre-stretch' refer to the same quantity, λ_Q. In the literature the term *pre-strain* is commonly employed; however, the term 'pre-stretch' is consistent with the fact that energy and stress functions are commonly presented with the principal stretches λ_i as variables.

The stress on the endplanes of the actuator, T_{11}, is also indicated in figure 2. This is the stress with which the actuator

may affect its surroundings. The measurable force with which the actuator works on its surroundings is

$$F_1 = x_2 x_3 T_{11} = \frac{x_2' x_3' T_{11}}{\lambda_1} = \frac{x_2 x_3' T_{11}}{\lambda_1 \lambda_Q}. \tag{2}$$

The last form is used for comparison of actuators of the same actual width x_2, but different pre-stretch λ_Q.

2.2. Measures of actuation

Two measures of actuation will be employed, defined by the condition under which they occur. The 'hanging weight' condition is referred to as the *constant load* or *isotonic* condition. A different measure of actuation output is termed the *blocked force* or *isostrain* condition. This is the force F_1 when the actuator length is kept constant, measured on the endplane with area $x_2 x_3$, as in (2). The endplane force is the physically measurable force which can be exerted on an external load, such as a suspended mass or a hinge in an active structure [18].

The results of an isotonic actuator test can be presented by plotting the deformation ratio of the actuator for given values of applied load and voltage, $\lambda_1(F_1, V)$. The actuator length x_1 and stretch λ_1 are always proportional. A plot of the actuation strain ξ reveals more of the actuation properties; it is defined as [24, 25]

$$\xi(F_1, V) = \frac{x_1(F_1, V) - x_1(F_1, 0)}{x_1(F_1, 0)}, \tag{3}$$

which is a comparison of the actuated to the unactuated length of the actuator, at the same load force. The actuation strain can also be presented using the intensive variables T_{11} and E (see table 2), by which the previous definition, (3), becomes

$$\xi(T_{11}, E) = \frac{x_1(T_{11}, E) - x_1(T_{11}, 0)}{x_1(T_{11}, 0)}. \tag{4}$$

Due to the large deformations inherent in dielectric elastomer actuators, also during actuation, the structural features of plots of $\xi(F_1, V)$ and $\xi(T_{11}, E)$ are very different, as will be found later.

2.3. The Ogden model for hyperelastic mechanical stress

The mechanical stress on the endplane of the stretched actuator can be modelled with hyperelastic models such as the one proposed by Ogden [26]. Under pure shear conditions (1) the stress on the endplane of a cuboid actuator with pre-stretch in the Ogden model is written as

$$T_{11} = \sum_{p=1}^{N} \mu_p (\lambda_1^{\alpha_p} - \lambda_1^{-\alpha_p} \lambda_Q^{-\alpha_p}), \tag{5}$$

where N is the number of terms, and μ_p and α_p are material parameters which can be found by a fit to experimental data. The shear modulus (at infinitesimal strain) of the Ogden model material is

$$G = \frac{1}{2} \sum_{p=1}^{N} \mu_p \alpha_p. \tag{6}$$

With this constraint, an N-parameter model has $2N - 1$ free fit parameters. The Ogden model has been included in models of dielectric elastomer actuators [8, 12, 17, 19, 24, 25], several of which have been verified experimentally.

2.4. Maxwell stress in electro-elastomers

The actuation pressure P in a planar dielectric elastomer actuator was initially [27] described using the simple expression $P = \varepsilon_0 \varepsilon_r E^2$, where ε_0 is the vacuum permittivity of free space, ε_r represents the relative permittivity of the material and E is the electric field, applied in the thickness direction (axis 3). This electrostatic pressure, commonly known as the Maxwell stress, can be written using tensor notation as

$$\sigma_{ij}^{(\mathrm{elec})} = \tfrac{1}{2}\varepsilon_0(2\varepsilon_r - a_1)E_i E_j - \tfrac{1}{2}\varepsilon_0(\varepsilon_r + a_2)E^2 \delta_{ij}. \tag{7}$$

The electrostrictive coefficients a_1 and a_2 were calculated for an isotropic polar rubber, and found to be of little importance in the case of low dielectric constant elastomers [28]; hence we will neglect their contribution, such that

$$\sigma_{ij}^{(\mathrm{elec})} = \tfrac{1}{2}\varepsilon_0 \varepsilon_r E_i E_j - \tfrac{1}{2}\varepsilon_0 \varepsilon_r E^2 \delta_{ij} \tag{8}$$

adequately describes the electrostatic stress in this case. A thorough discussion of the nature of electrostatic stress in a dielectric [29] concluded that the simplified version of (7) does represent the electrostatic stress in the case of an incompressible, dielectrically isotropic material.

2.5. Total actuation stress with boundary conditions

The total external stress on the actuator is balanced by the hyperelastic and Maxwell stresses in the material, by which static equilibrium can be described by

$$T_{ij} = \sigma_{ij}^{(\mathrm{elast})} + \sigma_{ij}^{(\mathrm{elec})} - p\,\delta_{ij}, \tag{9}$$

where T_{ij} is the total stress on the surfaces of the actuator, $\sigma_{ij}^{(\mathrm{elast})}$ and $\sigma_{ij}^{(\mathrm{elec})}$ are the elastic and the Maxwell stresses, respectively, while p is the external pressure. Eliminating p in (9), the total external stress on the endplane is found to be

$$T_{11} = \sigma_{11}^{(\mathrm{elast})} + \sigma_{11}^{(\mathrm{elec})} - \sigma_{33}^{(\mathrm{elast})} - \sigma_{33}^{(\mathrm{elec})} \tag{10}$$

$$\hat{=}\ T_{11}^{(\mathrm{elec})} + T_{11}^{(\mathrm{elast})}. \tag{11}$$

The form of this equation suggests that the internal stresses could be separated and somehow 'measured' on the endplane $x_2 x_3$; this will be discussed later.

The expressions for the hyperelastic and the Maxwell stresses ((5) and (8)) are inserted in (11), which results in the following expression:

$$T_{11} = -\varepsilon_0 \varepsilon_r E^2 + \sum_{p} \mu_p (\lambda_1^{\alpha_p} - \lambda_1^{-\alpha_p} \lambda_Q^{-\alpha_p}). \tag{12}$$

This expression is a constraint on the three intensive variables T_{11}, E and λ_1, thus leaving two free variables. This equation is highly nonlinear, which makes it impossible to isolate the variable λ_1 analytically, which is however possible using numerical tools. Here, the Mathematica 6 routine FindRoot was employed for the purpose. For the parameter ranges

investigated here, the routine always found unique solutions for the actuation stretch λ_1.

As discussed above, it may be useful to describe actuation in terms of the extensive variables F_1 and V in place of the intensive variables T_{11} and E. Especially for applications it may be practical to present results in terms of the extensive variables. The exchange is facilitated by direct replacement, using (2) for the replacement of endplane stress T_{11} with endplane force F_1, while the electrical field E can be replaced by the applied voltage through

$$E = \frac{V}{x_3} = \frac{\lambda_1 \lambda_Q V}{x_3'}. \tag{13}$$

When the replacement is carried through, the following force-balancing equation is obtained:

$$F_1 = -\frac{\varepsilon_0 \varepsilon_r x_2 \lambda_Q}{x_3'} \cdot \lambda_1 V^2 + \frac{x_2 x_3'}{\lambda_Q} \sum_p \mu_p (\lambda_1^{\alpha_p - 1} - \lambda_1^{-\alpha_p - 1} \lambda_Q^{-\alpha_p}). \tag{14}$$

This equation can be understood as a balancing of the forces acting on the endplane with area $x_2 x_3$.

The derived model and similar models can be expanded to include time-dependent behaviour, such as Newtonian motion [30], visco-elasticity [8, 17, 30] and dielectric dispersion. The mechanical and electrical properties of the electrodes have been disregarded; they may also be included [25, 31, 32]. However, the model captures the static equilibrium behaviour of the cuboid dielectric elastomer actuator, even without including these complications, as was demonstrated in [25].

3. Material parameters for the acrylic elastomer VHB 4910

The acrylic pressure sensitive glue VHB 4910 (produced by 3M) was found by Pelrine *et al* to have very useful properties for actuation [5, 6], and has therefore spurred much interest from others [4, 7, 8, 12, 17]. This material shows the typical hyperelastic traits in the force–stretch behaviour, namely, an initial linear region of higher stiffness, followed by a *plateau* region where the slope of the stress–stretch curve drops, ending with a *stretch-hardening* region in which the slope increases strongly (stretch-hardening is more commonly known as *strain-hardening*, however; stretch is used here as the main variable). The properties of this material are used in the following calculations on the actuation properties of the dielectric elastomer actuator.

3.1. Comparison of previous investigations

Several studies have been made to determine the material parameters of the VHB 4910 material, including parameters used in the Ogden model, some of which have been presented in table 1 (I–IV). The material parameters were determined from uniaxial experiments directly [12, 19], or they were inferred from electromechanical experiments [21]. For each set of parameters, the chosen strain rate $\dot{\lambda}$ of the test is presented, the shear modulus has been calculated using (6) and the resulting uniaxial stress–stretch curves have been plotted in figure 3.

Table 1. Ogden parameters of vulcanized natural rubber (I), and VHB 4910 (II–V). The value of K is discussed in the text.

	μ_p (kPa)	α_p	$\dot{\lambda}$ (% s^{-1})	G (kPa)	Reference
I	43.56	1.445	0.033	31.7	[12]
	0.117	4.248			(low rate)
II	112.2	1.450	9.4	81.3	[12]
	1.045×10^{-4}	8.360			(high rate)
III	8.58	1.293	0.33	73.7	[21]
	84.3	2.3252			($\varepsilon_r = 4.7$)
	−23.3	2.561			
IV	$-K$	1	2	$\frac{1}{2}K$	[19]
	K	2		17.5	($K = 35$ kPa)
V	92.29	1.130	2	52.2	
	0.01682	5.343			

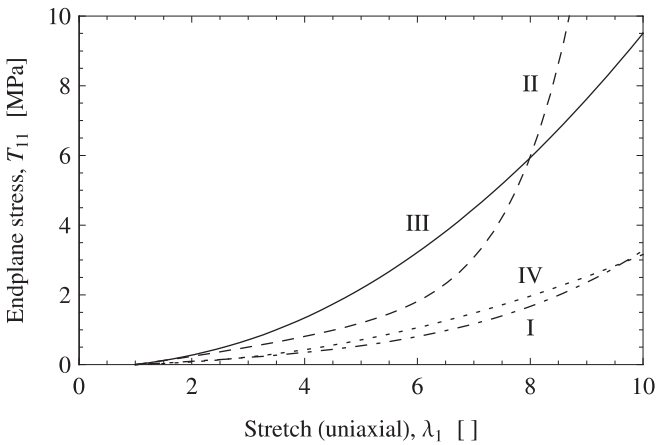

Figure 3. Plots of the stress T_{11} under uniaxial conditions, for the Ogden model parameters given in table 1.

The curves in figure 3 show large differences among them. Curves I and IV lie very close, although the strain rate for curve IV was 61 times larger than that for curve I. The curve marked III lies close to 3 times higher than curves I and IV, but with an intermediate strain rate. Curve II was obtained with a very high strain rate, 28 times higher than that for curve III; however, only for high stretch does curve II show higher stress than curve III. Curves I and II are from the same study, finding that an increased strain rate results in an overall higher stress at the same strain. However, this small meta-study shows that with the results presented in the literature so far, it is not possible to correlate independently obtained stress–stretch results well with strain rates. Most likely, other experimental factors were of greater influence, such as temperature during measurement (which would have a large influence on the perceived stiffness of the material), time of purchase of the material (see next paragraph), storage time of the purchased material, preparation and history of test samples, method of extraction of data (see previous paragraph), etc. Finally, it should be noted that the calculated shear modulus also does not correlate well with the overall progression of the stress–stretch curve. For instance, curve I presents a shear modulus

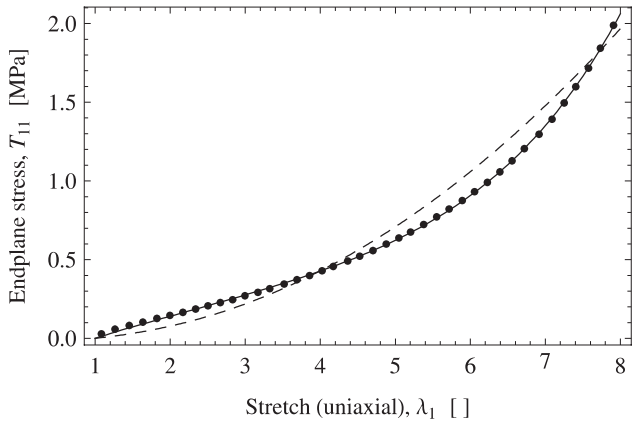

Figure 4. Plots of the results of a uniaxial stress–stretch experiment [19] (●). The curve for the fit parameters of the simplified fit is shown (table 1.IV, dashed), as well as that of the detailed four-parameter fit suggested here (table 1.V, full).

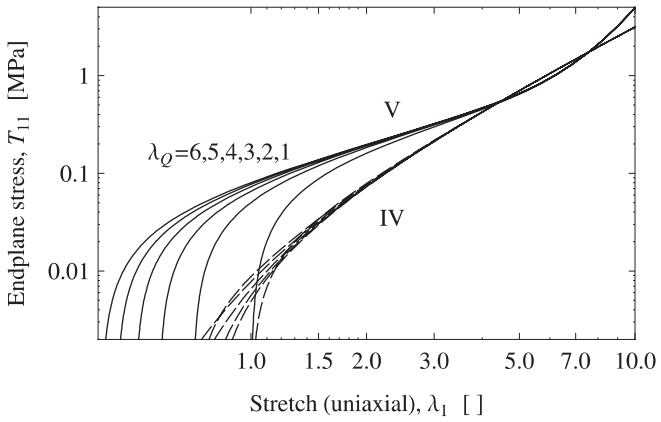

Figure 5. Pure shear stress–stretch curves for the Ogden parameters of the simplified fit (IV, dashed) and the detailed fit (V, full lines).

which is twice as large as that of curve IV, although they are very close when plotted. Thus, the shear modulus is not a good indicator of the high-stretch progression of the stress–stretch curve.

As discussed by Wissler and Mazza [22] the VHB 4910 material has probably changed its composition since it was first used for dielectric elastomer actuators in 2000 [5]. Changes in composition will affect the elastic properties as well as the dielectric properties. Dielectric spectroscopy measurements carried out in 2000 [33] on VHB 4910 under various conditions of strain showed the dielectric constant to be 4.7 at no strain, slightly dropping with increasing strain. Later measurements published in 2007 [22] likewise found a dielectric constant of 4.7 at no strain, but dropping dramatically with strain to 2.6 at $\lambda_1\lambda_2 = 25$. For simplicity, in the following it is assumed that the dielectric constant is 4.7 for the VHB 4910 material.

The material parameters of table 1.IV derive from a simplified 2-term Ogden model [19]. It reduces the number of free parameters to just one, K, by fixing parameters $\alpha_1 = 1$ and $\alpha_2 = 2$. This 'one-parameter' model was suggested in [19], and fitted to data obtained by a uniaxial stress–stretch experiment presented in the same paper. Presently, the data were extracted from figure 3 of that paper and presented here in figure 4 (filled circles, ●), together with the simplified fit suggested in the paper (dashed curve), with $K = 35$ kPa. Also shown is a 2-term, four-parameter fit (full curve), the parameters of which are presented in table 1.V (fit performed in Mathematica 6, with the NonlinearRegress routine). As can be seen from figure 4, the simpler fit captures the overall development of the curve, while the detailed fit with four free fit parameters follows the measured data more accurately, as is to be expected. The 'Estimated Variances' (provided by the NonlinearRegress routine) were 7.8×10^9 and 5.0×10^7 for the simplified and the more detailed fits, respectively.

It could be said that the simplified fit captures the general development of the stress, while only the detailed fit captures the progression fully. The highest value among the exponents α_i for the simplified fit was 2, which is apparently not enough to capture the stretch hardening, for which an exponent of $\alpha_2 = 5.343$ was seen to be necessary. In Ogden's original work [26], a three-term fit was used to fit stress–stretch data for a sulfur-vulcanized natural rubber, where it was found that an exponent of $\alpha_3 = 5.0$ could fit the stretch-hardening region well. It seems likely that at least one Ogden exponent must be high (≈4 and higher) in order to model stretch-hardening properly.

3.2. The effect of width pre-stretch on stress–stretch behaviour

As a first step in the investigation of the influence of pre-stretch on actuator performance, the effects of pre-stretch λ_Q on the mechanical properties are now investigated. Introduction of pre-stretch requires the use of pure shear boundary conditions (equation (1)), instead of the uniaxial boundary conditions employed previously in section 3. In figure 5, the effects are shown for the same set of parameters as for figure 4 (note that a double-logarithmic plot was used). It is seen that the pre-stretch mainly affects the initial region of stretch, from below $\lambda_1 = 1$ up to $\lambda_1 = 2$. The effect of pre-stretch can be found from 5, evaluated at $\lambda_1 = 1$,

$$T_{11}|_{\lambda_1=1} = \sum_{p=1}^{N} \mu_p (1 - \lambda_Q^{-\alpha_p}), \tag{15}$$

which only vanishes when $\lambda_Q = 1$.

From figure 5 and (15) two main effects of the pre-stretch on the stress–stretch curve can be observed: the stretch at which the endplane stress vanishes is shifted towards lower values, while all curves are seen to coalesce at higher stretches. It has been suggested that the effect of width pre-stretch is to 'stiffen' the material in the direction perpendicular to actuation [5]. Figure 5 shows that this is only the case when the stretch is below 2 and the stress is below 200 kPa, both values which are below the normal region of use for pre-stretched actuators. It must therefore be concluded that pre-stretch in the width direction mostly has no effect on the stress–stretch behaviour of a dielectric elastomer actuator in the actuation direction.

The force–stretch behaviour is also affected by pre-stretch, as illustrated in figure 6. These plots have been made with identical *final* actuator width $x_2 = 100$ mm. Again both the

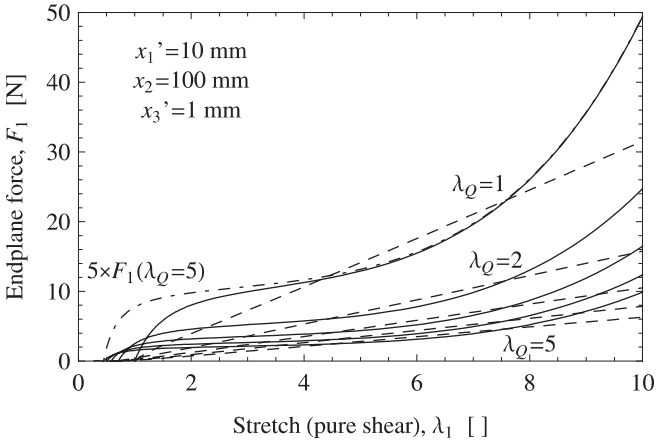

Figure 6. Pure shear force–stretch curves for the Ogden parameters of the simplified fit (IV, dashed) and the detailed four-parameter fit (V, full lines). The curve for the four-parameter fit with $\lambda_Q = 5$ was multiplied by 5 (dotted–dashed curve).

simplified and the four-parameter fits are shown, with dashed and full curves, respectively. As the pre-stretch is increased, the corresponding force at a given stretch is seen to drop. The curves for the simplified fit (IV) appear almost linear, while for the four-parameter fit (V) they appear curved, clearly showing that the simplified fit captures neither the plateau region, nor the stretch-hardening region.

Since we wish to investigate the influence of pre-stretch on the actuation, the passive mechanical properties of the actuators are sought to be made comparable. It was observed that when the force–stretch curve of the four-parameter fit with $\lambda_Q = 5$ was multiplied by 5, it was made to overlap well with the curve for $\lambda_Q = 1$. Geometrically, this would correspond to comparing actuators of identical *initial* width, which will be carried out by using x_2' as a parameter in the model, (14), such that it now reads

$$F_1 = -\frac{\varepsilon_0 \varepsilon_r x_2' \lambda_Q^2}{x_3'} \cdot \lambda_1 V^2 + x_2' x_3' \sum_p \mu_p (\lambda_1^{\alpha_p - 1} - \lambda_1^{-\alpha_p - 1} \lambda_Q^{-\alpha_p}) \quad (16)$$

by which the effect of differences in force–stretch behaviour are minimized, and the direct effects upon actuation are emphasized. In the following, the dimensions of the actuator are chosen as $x_1' = 10\,\text{mm}$, $x_2' = 100\,\text{mm}$ and $x_3' = 1\,\text{mm}$.

4. Evaluation of the cuboid actuator

The model of the cuboid dielectric elastomer actuator, in its intensive or extensive form (equations (12) and (14)) is entirely analytical, consisting of a single equation which determines a third variable from two independent variables (for instance λ_1 from a given set of T_{11} and E). It includes a number of materials and geometrical parameters, which can all be determined via separate independent experiments, and thus the model has no free fitting parameters. In table 2 a short overview of variables and parameters are presented; the parameters of the model of elasticity were chosen from the Ogden model of elasticity; however, any model of elasticity can be chosen, including Yeoh and Mooney–Rivlin types [8].

Table 2. Choice of variables for the cuboid actuator model. The variable transformations are given in equations (2) and (13).

	Variables	
	Intensive	Extensive
Extension	λ_1	x_1
Electrical	E	V
Boundary condition (load)	T_{11}	F_1
	Parameters	
Dimensions		x_1', x_2', x_3'
Elastic		$\{\mu_p, \alpha_p\}$
Permittivity		ε_r

In the following, plots of the actuation behaviour for both intensive and extensive variables are presented, under conditions of both blocked and constant stress, and blocked and constant load. The hyperelastic stress will be modelled using the detailed fit (table 1.V, 'detailed fit' in the following), comparing the results in places with those of the simplified fit (table 1.IV, 'simplified fit' in the following). The dielectric constant is taken to be $\varepsilon_r = 4.7$ and to be independent of strain (i.e. no electrostriction). In the case of extensive variables, the initial sample dimensions are taken as length $x_1' = 10.0\,\text{mm}$ and thickness $x_3' = 1.00\,\text{mm}$, corresponding to actuators made from the material VHB 4910. Initially, actuation presented with actuators of identical width *after* pre-stretch will be chosen, such that $x_2 = 100\,\text{mm}$. It will then be argued that a proper comparison follows between actuators of identical width x_2' *before* pre-stretch.

4.1. Intensive variables: blocked stress

The stress as a function of electric field is shown in figure 7. The top-most plot represents actuators that have no pre-stretch, $\lambda_Q = 1$, the full curves correspond to the simplifed fit while the dashed curves correspond to the detailed fit. All the curves are identical, except for differences in offset due to elastic stress. Inspecting one curve, for instance the dashed curve with $\lambda_1 = 4$, it is seen that the stress on the endplane drops when the electric field increases, a mode of action which is inherent to dielectric elastomer actuators. In physical terms, the Maxwell pressure is compressive in the thickness (3-axis) direction and works counter to the tensile stress, which is compressive in the other two directions (1- and 2-axes), hence the application of an electric field works to diminish the stress on the endplane. Further, all curves are seen to intersect with the abscissa, for an electric field at which the actuator would slacken and not be able to affect its surroundings. The area between the curve and the abscissa thus defines the range of operation at a given stretch configuration $\{\lambda_Q, \lambda_1\}$. Finally, it should be observed that the differences between the simplified and the detailed fit do not appear of great importance in this plot.

The lower plot in figure 7 shows the same curves as the upper plot, only the abscissa is plotted with electric field squared, E^2. It is seen that the plotted curves are all linear and have different offsets depending upon the stretch λ_1. As

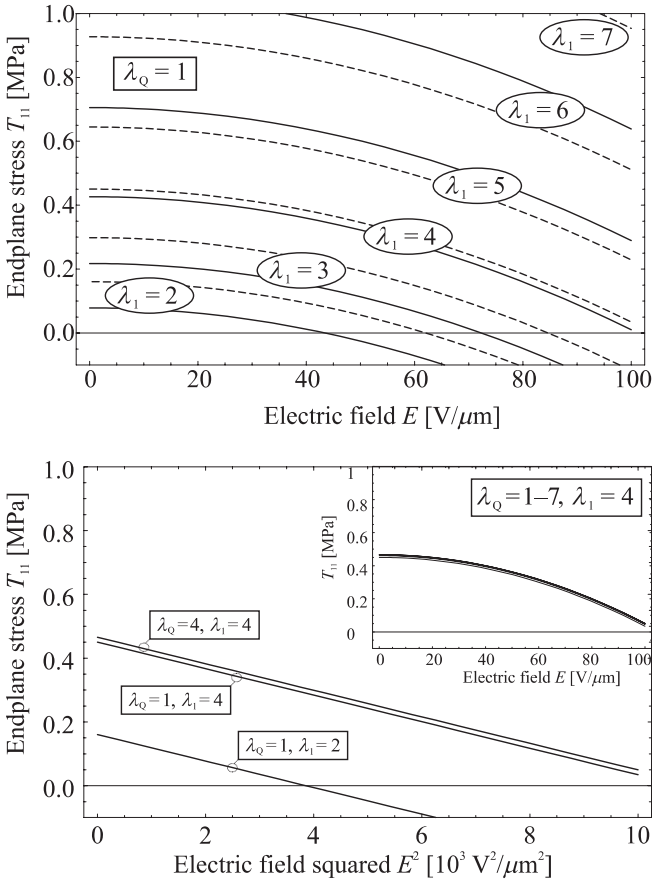

Figure 7. Blocked stress of the cuboid actuator under various conditions of stretch. The upper plot shows curves for $\lambda_Q = 1$, under different conditions of length stretch λ_1, the full curves are for the simplified fit, the dashed curves for the detailed fit. The lower plot details features of the upper plot.

can be observed, a change in stretch λ_1 influences the offset of the curves strongly, while a change in pre-stretch λ_Q has a vanishing effect upon the offset. The inset shows that the blocked stress curves for a stretch $\lambda_1 = 4$ and varying pre-stretches are almost indistinguishable.

The case that the curves become linear in a plot of endplane stress versus electric field squared can be seen directly from the model (equation (12)),

$$\left.\frac{\partial T_{11}}{\partial (E^2)}\right|_{\lambda_1, \lambda_Q} = -\varepsilon_0 \varepsilon_r. \tag{17}$$

This fact has the important consequence that a simple and accurate independent measurement of the dielectric constant at a predetermined stretch configuration $\{\lambda_Q, \lambda_1\}$ can be made. Equation (17) shows that the blocked stress of a cuboid actuator depends only on the dielectric constant of the material. With this approach, the property of electrostriction (the particular variation of dielectric constant with strain) could be measured directly. The approach has been demonstrated experimentally in the case of a VHB 4910 cuboid actuator [6] and a silicone cuboid actuator with no pre-stretch [25].

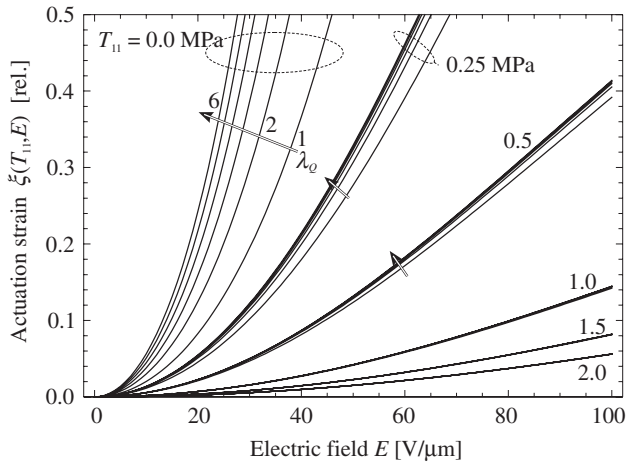

Figure 8. Actuation strain curves for various conditions of pre-stretch λ_Q and endplane stress T_{11}. Curves for equal endplane stress cluster together.

4.2. Intensive variables: actuation strain

The actuation strain curves with constant endplane stress are presented in figure 8. For each value of the endplane stress, curves for pre-stretches $\lambda_Q \in \{1, 2, 3, 4, 5, 6\}$ have been plotted. In the special case of no applied endplane stress it is seen that the pre-stretch has a large improving effect upon the actuation strain. In the more general case of a finite endplane stress, the pre-stretch is found to have a minimal effect upon the position of the actuation strain curve. Finally, it is seen that an increase in the endplane stress has the effect of drastically lowering the actuation strain at a given electric field.

The above plots of the actuation behaviour with the use of intensive variables T_{11} and E reveal that pre-stretch does not affect the electromechanical coupling directly. However, there are other properties of the actuation which are affected by pre-stretch; most notably, it has been shown experimentally [7, 12] that pre-stretch has the effect of increasing the electric breakdown field, up to one order of magnitude. Recently, it has been attempted to explain this effect via a thermodynamic stability criterion [15]. Presently, we shall only deal with the direct effects of pre-stretch on actuation of the cuboid actuator, disregarding any practical limits on the applicable electric fields.

4.3. Extensive variables: blocked force

The blocked force surfaces for the detailed fit are presented in figure 9 for six different pre-stretches $\lambda_Q \in \{1, 4, 6\}$, with voltage V and actuator stretch λ_1 as variables. For a pre-stretch of $\lambda_Q = 1$, the blocked force is hardly affected by the applied voltage (ranging from 1 to 5 kV). With a pre-stretch of $\lambda_Q = 4$, the effect of the voltage becomes visible, causing a reduction of the force on the endplane of the cuboid actuator. It is interesting to note that the force reduction becomes more pronounced as the actuator stretch λ_1 increases. Finally, for a pre-stretch of $\lambda_Q = 6$, the voltage effects become even more pronounced, in parts of the plot resulting in a complete cancellation of the blocked force.

When extensive variables are employed instead of intensive variables, applications-oriented consequences

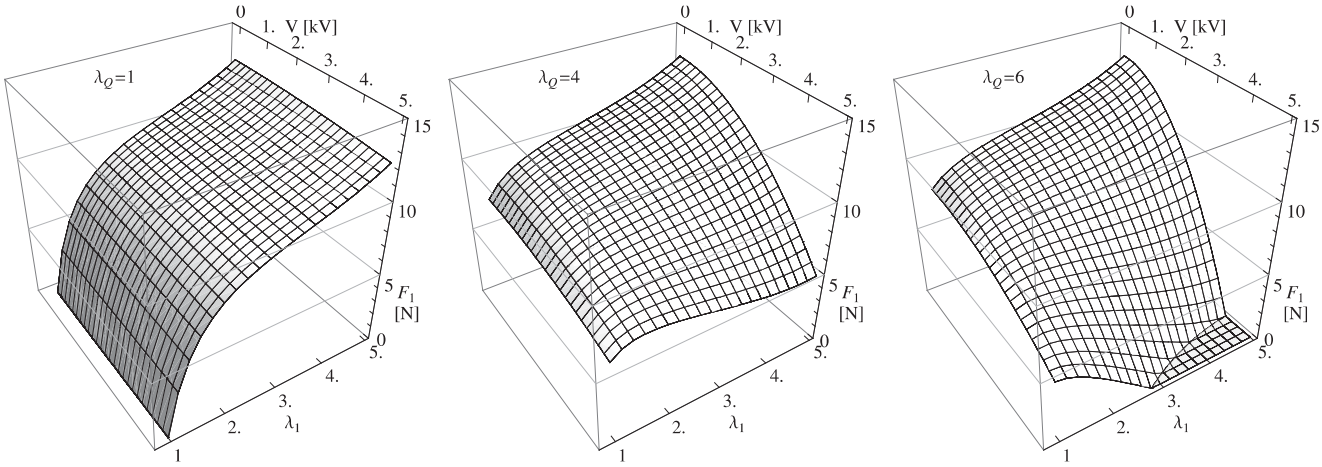

Figure 9. Blocked force surfaces for the detailed fit. The six plots are for three different pre-stretches, $\lambda_Q \in \{1, 4, 6\}$.

become more obvious. In experiments and for device applications, it is the voltage V and the endplane force F_1 which can be controlled, not the stress T_{11} or the electric field E. The dimensions and the range of voltages and forces employed in figure 9 are typical for experiments with VHB 4910 as dielectric material. The plots show that *both* pre-stretch λ_Q and stretch λ_1 must be on the order of 4 to 5, to enable a large variation in the blocked force, under the given conditions. For instance, for the $\lambda_Q = 4$ plot, a 50% drop in the blocked force in going from 0 to 5 kV can be found only when $\lambda_1 \approx 4$ and above.

4.4. Extensive variables: actuation strain

The actuation strain (3) for the actuation model with extensive variables F_1 and V (equation (16)) is presented in figure 10, for typical applied voltages V and force loads F_1. The top row of plots corresponds to calculations based on the simplified model, the bottom row to the detailed model. From left to right, the pre-stretch increases from 1 to 5. The actuation strain scale is the same for all plots, from $\xi = 0$ to 1, to ease comparison between plots. For all plots, the actuation strain increases with increasing voltage.

Focussing first on the top row of plots of the actuation strain for the simplified fit, it is found that the actuation strain output strongly increases with pre-stretch. It is also found that the influence of the load is almost negligible. For a pre-stretch of $\lambda_Q = 5$, the actuation strain is close to 1 (100% increase in actuator length) for all loads.

The actuation strain plots for the detailed fit (bottom row) look very different from those of the simplified fit. As the width pre-stretch increases, the actuation strain also increases; however, high actuation strains are found only in a certain region of the load F_1. This region could be identified as the 'optimum load' region [25], and a rough value of 10 N could be identified here as the optimum load.

From the force–stretch curves in figure 6 the occurrence of an optimum load region can be directly justified: the value of 10 N is found in the centre of the plateau region, around a stretch $\lambda_1 \approx 4$. In this region, the slope of the force–stretch curve is minimal, such that the additional Maxwell's stress may result in largest possible stretches. Conversely, it could therefore be argued that the effect of attaching an optimum load to the actuator is to introduce a stretch λ_1 in the actuation direction that brings the actuator 'working' stretch within the plateau region of the force–stretch curve. Therefore, in the direction of actuation strain, the stretch should be at least $\lambda_1 = 2$. Finally, the influence of pre-stretch on the value of the optimum load is negligible, as seen by comparison of the plateau regions of figure 6 with the regions of large actuation strain in figure 10.

Actuation strain measurements on VHB 4910 cuboid actuators made with pre-stretches $\lambda_Q = 4$, 5 and 6 were presented in [24] (stress–stretch measurements on VHB 4910 not available). These measurements showed behaviour almost identical to that displayed by the plots based on the detailed fit. The predicted positions of the optimum load were found consistently to be 3 times higher than measured, and the predicted actuation strains were also higher. The discrepancies can be explained by the very long time needed to complete an actuation strain experiment (after the application of a step voltage, considerable creep may be observed over a period of 1000 s [21]), causing the material to appear softer than what the stress–stretch model assumes, as it is based on a test that lasted only 450 s (table 1 and figure 4). Still, bar details, the experimental presence of the optimum load feature is clearly found also in the theoretical model.

Since the influence of visco-elastic behaviour is so pronounced for VHB 4910, it is to be expected that predictions for the VHB 4910 material (16) will not be precise; however, as the above comparison shows, the main features are still captured, and the above conclusions regarding the direct influence of pre-stretch on electromechanical properties of a dielectric elastomer actuator remain valid. The model will provide more precise predictions for elastomers with lower visco-elastic contribution, as was found in [25], where the model was shown to predict the actuation properties of a silicone cuboid actuator (without width pre-stretch), including the accurate position of the optimum load and to within 37% the maximum actuation strain at a given voltage.

The actuation of the cuboid actuator is influenced strongly by the pre-stretch; however, the electromechanical coupling is not affected directly, as was illustrated when investigating

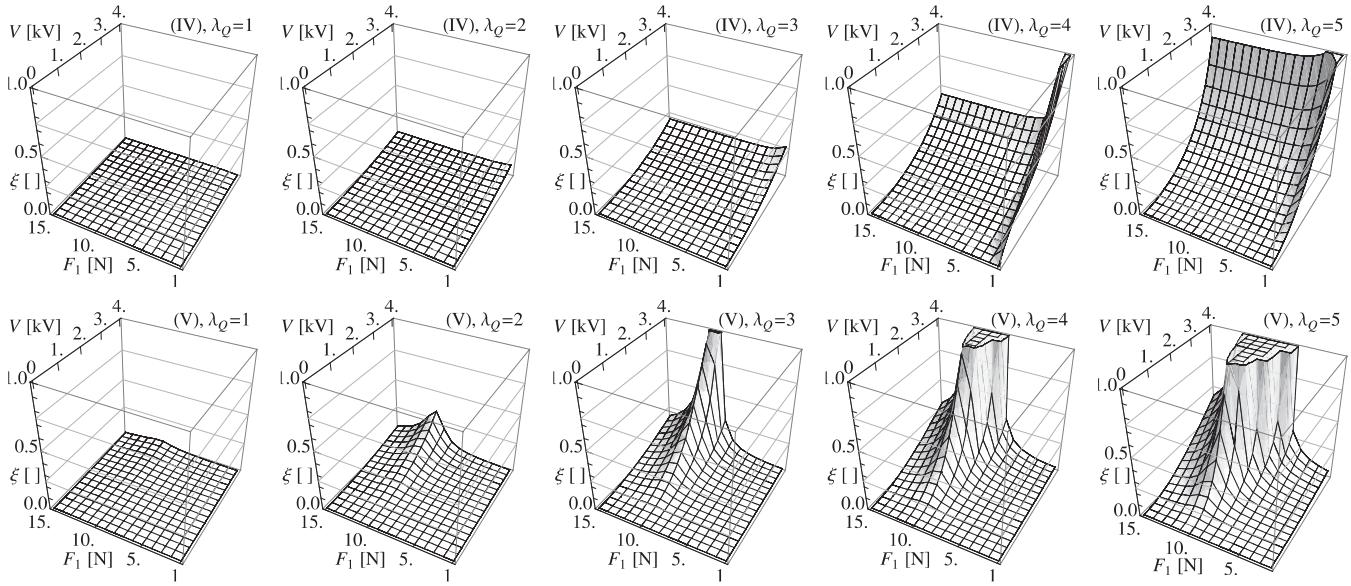

Figure 10. Actuation strain for the extensive variables load F_1 and voltage V. Both the simplified fit (IV) and the detailed fit (V) have been employed, for pre-stretches $\lambda_Q = 1, 2, 3, 4, 5$.

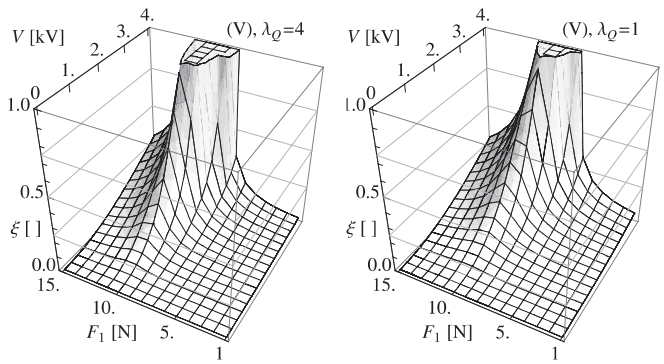

Figure 11. Actuation strain for actuators of identical dimensions, with pre-stretches $\lambda_Q = 4$ (left) and $\lambda_Q = 1$ (right).

the actuation properties using intensive variables. Instead, the effect of pre-stretch on the actuation of a device is through altering the geometry of that device, making it wider and thinner, such as to increase the Maxwell's stress at a given voltage. To emphasize that this is indeed the case, in figure 11 actuation strain plots for two actuators with almost identical *final* dimensions have been shown. The left-most graph was calculated for a pre-stretch of $\lambda_Q = 4$ and dimensions $x_2' = 100\,\text{mm}$ and $x_3' = 1\,\text{mm}$, as before. The right-most graph is for $\lambda_Q = 1$, while the dimensions were chosen as $x_2' = 4 \times 100\,\text{mm}$ and $x_3' = \frac{1}{4}\,\text{mm}$, such that the dimensions of the two actuators were almost similar for identical load force. As can be seen in figure 11, the two plots are close to identical, both in the position of the optimum load and in the overall size of the actuation strain.

5. Conclusion

The model for the actuation of a pure shear cuboid actuator with pre-stretch λ_Q was presented, including the variable transformations for shifting between intensive and extensive variables. The electromechanical coupling was provided by the Maxwell's stress, while the hyperelastic properties were represented with an Ogden model. The Ogden model was discussed in the case of the VHB 4910 material. Experimental results obtained by several researchers were compared, showing large discrepancies between the experimental results as well as the Ogden parameters obtained. The accuracy of a simplified fit [19] was discussed, the underlying data extracted and a more detailed four-parameter fit made.

The mechanical behaviour of pre-stretched elastomer material was mostly unaffected by pre-stretch, as was investigated via stress–stretch curves (intensive variables). It was also shown that devices of different pre-stretches have comparable force–stretch curves when they have identical *initial* dimensions x_i'.

The blocked stress was mostly independent of pre-stretch, but highly dependent upon stretch λ_1. It was shown that plotting the blocked stress against electric field squared, E^2, straight sloping lines were found, with a slope equal to the dielectric constant. This forms a method by which the dielectric constant, or, if present, electrostriction, can be quantified independently. Indeed, this method might help to shed light on the nature of Maxwell's stress.

The actuation strain was strongly affected by endplane stress; however, the effect of pre-stretch was less clear. For very low values of end-plane stress, the actuation strain curves for different pre-stretches were obviously separated; however, for endplane stresses typically found in applications, the actuation strain curves for different pre-stretches would be practically identical. In conclusion to the investigation of actuation in terms of intensive variables, it was therefore found that the influence of pre-stretch is negligible.

When employing extensive variables, the effects of pre-stretch are apparently strong. When no pre-stretch is introduced, the applied voltage could hardly affect the blocked force, while at higher pre-stretches the voltage could fully cancel it. This was especially the case when the stretch λ_1 was also high.

The actuation strain was calculated for both simplified and detailed fits. The simplified fit could not capture typical actuation strain behaviour for the cuboid actuator while the detailed fit could. An optimum load was identified, and seen to remain constant with varying pre-stretch, justifying the choice of using initial dimensions as the basis of comparison. It was found that the optimum load corresponds to the plateau region of the force–stretch curve. Finally, it was demonstrated how two actuators of different pre-stretches, but identical *final* dimensions would display almost identical actuation strain behaviour curves. This discovery could be of great importance to the proper design of actuating structures.

As an important side remark, it should be pointed out that the actuation strain behaviour presented by the simplified fit would be desirable, since for all pre-stretches the actuation strain is found to be practically independent of load. With such simplified actuation behaviour, the design of robots and active structures based on these actuators would be greatly simplified. Materials scientists might be able to design elastomer systems that have this force–stretch behaviour. It is recommendable to have the force–stretch curve end with strong stretch-hardening (by achieving one Ogden parameter $\alpha \leqslant 4$) in order to avoid the electromechanical instability that leads to breakdown [15]. This might be achievable with inter-penetrating networks [34].

Dielectric elastomer actuation evaluated under intensive variables is not influenced by pre-stretch, whereas under extensive variables the influence appeared strong. However, using extensive variables it was found that if an actuator without pre-stretch was prepared with the same dimensions as those of a pre-stretched actuator, their actuation strain would be almost indistinguishable. The conclusion must be that, while the electromechanical coupling is unaffected by pre-stretch, the alteration of the dimensions of the actuator renders it more practically useful towards applications in that activation voltages are lowered.

It must be emphasized that pre-stretch results in other important effects of importance to actuation, principally that of strongly increasing the breakdown strength, in some cases by more than an order of magnitude. Also, the incorporation of pre-stretch can allow useful structures capable of push–pull actuation. The occurrence of optimum load suggests that to obtain large actuation strains, actuators and actuating structures must operate in the plateau region. For typical elastomers, this corresponds to tuning the initial stretch to $\lambda_1 = 3$ to 5.

In summary, in general terms the effect of width pre-stretch is to make the material thinner and to increase the electrical breakdown strength. The optimum load stretches the actuator far enough to place its operation in the plateau region, which softens the material and allows larger actuation strain. These conclusions could improve the understanding of any type of dielectric elastomer actuator incorporating pre-stretch.

The above investigation has helped to clarify the role of pre-stretch in dielectric elastomer actuation, as affecting actuator geometry almost without interfering with the electromechanical coupling. It remains to be seen how well the conclusions will hold for more complex materials, such as polymer blends, partially crystalline elastomers and composite materials; however, if the mechanical and dielectric properties can be measured independently, it should be possible to apply the principle of total stress, (9), here as well. In the cases of electrostriction, in which the dielectric properties explicitly change with strain, or of nonlinear dielectric properties, in which the dielectric properties change with applied electric field [35], the pre-stretch should affect the electromechanical coupling directly; however, the presented analysis will work well for dielectrically isotropic elastomers with low visco-elastic components and the conclusions drawn above should remain valid for all such materials.

Acknowledgments

The author acknowledges the support from the WING initiative of the Germany Ministry of Education and Research through its NanoFutur program (Grant No NMP/03X5511). The author thanks Matthias Kollosche, Bernhard Mokross and Reimund Gerhard for valuable discussions.

References

[1] Bar-Cohen Y (ed) 2004 *Electroactive Polymer (EAP) Actuators as Artificial Muscles: Reality, Potential, and Challenges* (Bellingham, WA: SPIE Press)

[2] Carpi F, De Rossi D, Kornbluh R, Pelrine R and Sommer-Larsen P (ed) 2008 *Dielectric Elastomers as Electromechanical Transducers* (Amsterdam: Elsevier)

[3] Pelrine R, Kornbluh R, Joseph J, Heydt R, Pei Q and Chiba S 2000 High-field deformation of elastomeric dielectrics for actuators *Mater. Sci. Eng.* C **11** 89–100

[4] Lochmatter P, Kovacs G and Wissler M 2007 Characterization of dielectric elastomer actuators based on a visco-hyperelastic film model *Smart Mater. Struct.* **16** 477–86

[5] Pelrine R, Kornbluh R, Pei Q and Joseph J 2000 High-speed electrically actuated elastomers with strain greater than 100% *Science* **287** 836–9

[6] Pelrine R, Kornbluh R and Kofod G 2000 High-strain actuator materials based on dielectric elastomers *Adv. Mater.* **12** 1223–5

[7] Kofod G, Sommer-Larsen P, Kornbluh R and Pelrine R 2003 Actuation response of polyacrylate dielectric elastomers *J. Intell. Mater. Syst. Struct.* **14** 787–93

[8] Wissler A and Mazza E 2005 Modeling of a pre-strained circular actuator made of dielectric elastomers *Sensors Actuators* A **120** 184–92

[9] Kovacs G, Lochmatter P and Wissler M 2007 An arm wrestling robot driven by dielectric elastomer actuators *Smart Mater. Struct.* **16** S306–17

[10] Pei Q, Pelrine R, Stanford S, Kornbluh R D and Rosenthal M S 2003 Electroelastomer rolls and their application for biomimetic walking robots *Synth. Met.* **135–136** 129–31

[11] Wingert A, Lichter M D and Dubowsky S 2006 On the design of large degree-of-freedom digital mechatronic devices based on bistable dielectric elastomer actuators *IEEE/ASME Trans. Mechatronics* **11** 448–56

[12] Plante J-S and Dubowsky S 2006 Large-scale failure modes of dielectric elastomer actuators *Int. J. Solids Struct.* **43** 7727–51

[13] Kofod G, Wirges W, Paajanen M and Bauer S 2007 Energy minimization for self-organized structure formation and actuation *Appl. Phys. Lett.* **90** 081916–3

[14] Lochmatter P, Kovacs G and Ermanni P 2007 Design and characterization of shell-like actuators based on soft dielectric electroactive polymers *Smart Mater. Struct.* **16** 1415–22
[15] Zhao X and Suo Z 2007 Method to analyze electromechanical stability of dielectric elastomers *Appl. Phys. Lett.* **91** 061921
[16] Goulbourne N C, Mockensturm E M and Frecker M I 2007 Electro-elastomers: large deformation analysis of silicone membranes *Int. J. Solids Struct.* **44** 2609–26
[17] Goulbourne N, Mockensturm E and Frecker M 2005 A nonlinear model for dielectric elastomer membranes *J. Appl. Mech.* **72** 899–906
[18] Lochmatter P and Kovacs G 2008 Design and characterization of an active hinge segment based on soft dielectric eaps *Sensors Actuators* A **141** 577–87
[19] Lochmatter P, Kovacs G and Silvain M 2007 Characterization of dielectric elastomer actuators based on a hyperelastic film model *Sensors Actuators* A **135** 748–57
[20] Mockensturm E M and Goulbourne N 2006 Dynamic response of dielectric elastomers *Int. J. Non-Linear Mech.* **41** 388–95
[21] Wissler M and Mazza E 2007 Mechanical behavior of an acrylic elastomer used in dielectric elastomer actuators *Sensors Actuators* A **134** 494–504
[22] Wissler M and Mazza E 2007 Electromechanical coupling in dielectric elastomer actuators *Sensors Actuators* A **138** 384–93
[23] Lochmatter P 2007 Development of a shell-like electroactive polymer (EAP) actuator *PhD Thesis* Swiss Federal Institute of Technology, Zürich
[24] Kofod G 2001 Dielectric elastomer actuators *PhD Thesis* Risø National Laboratory/Danish Technical University, Risø ISBN 87-550-2925-6
[25] Kofod G and Sommer-Larsen P 2005 Silicone dielectric elastomer actuators: finite-elasticity model of actuation *Sensors Actuators* A **122** 273–83
[26] Ogden R W 1972 Large deformation isotropic elasticity—on the correlation of theory and experiment for incompressible rubberlike solids *Proc. R. Soc. Lond.* A **326** 565–84
[27] Pelrine R E, Kornbluh R D and Joseph J P 1998 Electrostriction of polymer dielectrics with compliant electrodes as a means of actuation *Sensors Actuators* A **64** 77–85
[28] Yamwong T, Voice A M and Davies G R 2002 Electrostrictive response of an ideal polar rubber *J. Appl. Phys.* **91** 1472–6
[29] McMeeking R M and Landis C M 2005 Electrostatic forces and stored energy for deformable dielectric materials *J. Appl. Mech.* **72** 581–90
[30] Sommer-Larsen P, Kofod G, Shridhar M H, Benslimane M and Gravesen P 2002 Performance of dielectric elastomer actuators and materials *Smart Structures and Materials: Electroactive Polymer Actuators and Devices* vol 4695 ed Y Bar-Cohen (Bellingham, WA: SPIE) pp 158–66
[31] Carpi F, Chiarelli P, Mazzoldi A and de Rossi D 2003 Electromechanical characterisation of dielectric elastomer planar actuators: comparative evaluation of different electrode materials and different counterloads *Sensors Actuators* A **107** 85–95
[32] Keplinger C, Kaltenbrunner M, Arnold N and Bauer S 2008 Capacitive extensometry for transient strain analysis of dielectric elastomer actuators *Appl. Phys. Lett.* **92** 192903
[33] Kofod G, Kornbluh R D, Pelrine R and Sommer-Larsen P 2001 Actuation response of polyacrylate dielectric elastomers *Smart Structures and Materials: Electroactive Polymer Actuators and Devices* vol 4329 (Bellingham, WA: SPIE) ed Y Bar-Cohen pp 141–7
[34] Ha S M, Yuan W, Pei Q, Pelrine R and Stanford S 2006 Interpenetrating polymer networks for high-performance electroelastomer artificial muscles *Adv. Mater.* **18** 887–91
[35] Robertson J and Hall D A 2008 Nonlinear dielectric properties of particulate barium titanate-polymer composites *J. Phys. D: Appl. Phys.* **41** 115407